(2)

Effects of Heating/Cooling on Changes in Sea Surface Temperature: Consequences for Computation of Surface Advection from Satellite Images

Annual Report

Principal Investigator:

Bill Emery
CCAR Box 431
Univ. of Colorado
Boulder, Co., 80309

Oct. 24, 1989

Introduction

The purpose of this project is to study the error sources in computing surface advection from sequential satellite images primarily focusing on the interpretation of infrared weather satellite-derived sea surface temperature (SST) images. To evaluate the effects of heating and cooling at the ocean's surface the FASINEX data set was acquired along with coincident AVHRR images of the same region. A simple study of the satellite temperatures and those measured at the FASINEX moorings suggests the advective nature of the surface temperature field. A more detailed model is now being developed to reveal in detail the relationship between the surface heat fluxes and the change of SST seen in the satellite images.

In addition we are presently studying simultaneous pairs of AVHRR and CZCS imagery to develop an understanding of the similarities and differences between surface motion computed from changes in SST patterns and motion computed from changes in ocean color as revealed by the CZCS instrument. Unfortunately we only have CZCS imagery available with 24 hour separations between images while the AVHRR can have separations as short as 4-6 hours. The shorter the interval the better the performance of the surface velocities computed from the AVHRR data.

While there are similarities between the AVHRR and CZCS data patterns there are also some marked differences between the two different types of imagery. The question is are these differences caused by the very different competing sources of local variation (ie, heat flux for SST and biological activity for CZCS) or by the advection changes of the

surface patterns that we are trying to track. More study is needed to quantify the differences/similarities between these two fields.

The attached report spells out some of the recent results of this project.

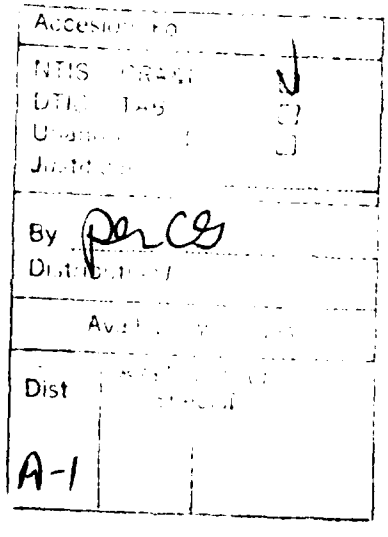

Effects of Heating/Cooling on Changes in Sea Surface Temperature; Consequences for Computation of Surface Advection from Satellite Images

A Preliminary Report

by
Bill Emery and Carol Anne Clayson
CCAR Box 431
Univ. of Colorado
Boulder, Co., 80309
ph 303-492-8591

Aug., 1989

Introduction

Recent research (Emery et al., 1986; Emery et al., 1989; Kamachi, 1989) has demonstrated the potential for computing sea surface motion from advective changes in satellite infrared sea surface temperature (SST) patterns. The critical assumption in this method is that all of the changes in SST observed by the satellite are caused by horizontal advection. In many cases this may be a valid assumption while in others it is clearly incorrect. The two primary competing mechanisms that can alter SST are surface heating/cooling and vertical advection (upwelling/downwelling). The potential contributions from vertical and horizontal mixing are suppressed by the relatively short intervals (6-24 hours) between the successive satellite images.

Of the two primary effects heating/cooling is the more pervasive and perhaps the more difficult to assess in its contribution to changes in satellite infrared SST patterns. We hope to estimate the contribution of heating/cooling to these changes by comparing heat flux terms, computed from the FASINEX data set (kindly provided by Bob Weller) with the SST patterns in coincident AVHRR imagery (kindly provided by Peter Cornillon). Weller's data set also makes it possible to directly compare satellite SST with near surface SST measurements and to compare image derived advective surface velocities with those directly measured by current meters near the surface (10m). The purpose of this short report is to provide collaborating scientists (Weller and Cornillon) with a preliminary view of some early comparisons between these two data sets, to describe our plan of attack and to solicit ideas from others as to what other steps might be taken to better understand the accuracy and reliability of the surface velocities inferred from the sequential satellite images. This report also serves as a interim progress report to Frank Herr at ONR.

Data

The data for this comparison consist of moored current, temperature and heat-flux measurements made at nine FASINEX moorings over roughly a six-month period at the beginning of 1986. A series of 25 AVHRR satellite images were also collected during this same time period from which 14 image pairs (intervals between images of 24 hours or less) were used to compute surface motion. The positions and dates of the FASINEX moorings are shown here in Tables 1 and 2 (Pennington et al. 1988). The dates of the corresponding satellite images are given in Table 3. The map in Fig. 1 displays the study area with the FASINEX moorings and defines the area within which the surface velocities were computed from the satellite images. Examples of the satellite images are presented here in Figs. 2 and 3 which both show the FASINEX area as an inset. From May, 1986 these two images are fairly clear of cloud cover in the FASINEX region. This combination of satellite and in situ data provide a very unique opportunity for evaluating the effects of heating/cooling on the SST pattern changes.

Preliminary Results

a. Surface Temperature Comparisons

One of the most direct comparisons made possible by this combination of satellite and in situ data is the comparison between the SST's measured from the mooring surface floats (at about 0.5 to 1.0 m down from the buoy waterline) and the calibrated satellite infrared temperature. All of the satellite imagery were routinely calibrated using the Multi-Channel SST (MCSST) method described by McClain et al. (1985) and thus were available as surface temperatures rather than as satellite brightness values.

A scatter diagram relating the buoy measured SST's with the corresponding satellite MCSST values are is presented here in Fig. 4. Also shown is the appropriate regression line and the interval of plus/minus one standard deviation. It is clear from this diagram that there is little correlation between these two different measurements of SST. The correlation, given at the top of the plot, is 0.3 which is quite low especially for two quantities that are supposed to be measures of the same thing.

The scatter points indicate that the buoy temperatures had a much smaller range (23.4 to 25.0 C) than the coincident satellite SST's (23.2 to 26.5 C). Part of this may be due to contributions from low clouds or from spurious small cloud patches. Clouds, however, would systematically bias the satellite SST's to lower values due to atmospheric absorption of infrared radiation emitted from the ocean. The symmetrical appearance of the scatter points, about the regression line suggests that this is not likely the explanation for the differences.

Another problem is the difference between satellite skin and buoy bulk SST measurements. As discussed in Schluessel et al., (1987) satellites measure skin temperature while buoys measure the bulk temperature about 1 m below the surface. This is the case with this FASINEX comparison and is also the calibration principal behind the MCSST. Thus skin-bulk differences between the satellite values and the buoy measured SST's could contribute to both positive and negative differences. Emery and Schluessel (1989) discuss how global skin versus MCSST differences can vary from -0.8 to +1.2 ^{o}C. Only a portion of the variability in Fig. 4 can be explained therefore by the skin versus MCSST differences.

b. Heat-flux Temperature Comparisons

Another instructive comparison is to compute the daily net heat exchange from the suite of moored FASINEX data (Pennington et al., 1988) and to compare these heat fluxes with the corresponding changes in satellite SST (Fig. 5). Here for example is the net heat-flux, computed at mooring F2 along with the satellite IR SST extracted at this same location for the appropriate times. It is interesting that the satellite SST's follow the same general trend seen in the net heat flux in that the SST's are declining over time at the same time that the net heat flux goes down. The final satellite SST value increases slightly as does the net heat flux. This was not always the case for all of the comparisons carried out but appears more than half the time.

A more important comparison is that between the net heat flux and the change in temperature between images in the pairs used to computer the horizontal advective velocities (Fig. 6). Here again are plotted the mean regression line along with the interval defined by the standard deviation. Note here that most of the points fall within this interval suggesting that there is likely some relationship between the changes in satellite SST and the net heat flux. Also the correlation value between the image temperature changes and the net heat flux, while not being very high, at 0.45 is much closer to 0.5. The low correlation is mostly due to a few points that stray wildly from the regression line. It may be these cases that are due more to horizontal advection than to local heating and cooling. This will be checked by selecting out those values which exceed the one-sigma limits from the regression line.

These differences can be viewed in another way as the histogram of differences between the satellite temporal SST changes and the net heat flux. Clearly most of the values lie near 0 with an equal sized peak at slightly greater positive values. Overall the bias appears to be towards

the lower values (negative values) but this is difficult to quantify.

c. Advective Surface Velocities

As an example of the surface velocities computed from the AVHRR images the vectors of Fig. 7 were computed from the pair of images presented here as Figs. 2 and 3. The locations of the FASINEX moorings are indicated on the plot of the surface advective currents. Typical of the region there is no strong, coherent surface flow and the current field is dominated by eddies and small regions of more intense flow. This surface current map is quite typical of some of the other flow fields inferred from the satellite image pairs. In a variable flow field like this it is difficult to distinguish the coherent ocean currents from the random influences of clouds. Applied to a series of Gulf Stream AVHRR images (Emery et al., 1989) this same technique is capable of extracting the strongest, most-coherent flows but only after a series of statistical significance and spatial coherence filters were applied.

Planned Future Comparisons

We intend to carry out a number of other direct comparisons including:

1. Compare directly measured near-surface (10 m) currents with those inferred from the satellite images.
2. Compute the horizontal heat advection from the moorings (T and V measurements) and compare with those inferred from the satellite imagery.
3. Develop a model of surface heat exchange to determine quantitatively what the SST change should be for the net heat flux measured at the FASINEX moorings.
4. Apply this model and subtract the SST change from the appropriate

satellite images and recompute the SST advective motion field. Compute the differences between this motion field and that without the heat flux correction and regard these differences as error limits on the surface velocities.

References

Emery, W.J., C.W. Fowler and C.A. Clayson, 1989: Satellite image derived Gulf Stream currents. submitted to J. Phys. Oceanogr.

Kamachi, M., 1989: Advective surface velocities derived from sequential images for rotational flow field: limitations and applications of maximum cross correlation method with rotational registration. submitted to J. Geophys. Res.

McClain, E.P., W.G. Pichel and C.C. Walton, 1985: Comparative performance of AVHRR based multichannel sea surface temperatures. J. Geophys. Res. 90, 11,587-11,601

Pennington, N.J., R.A. Weller and K.H. Brink, 1988: FASINEX moored current meter array data report, WHOI Tech. Rpt. 88-63, Woods Hole, Ma.

Schluessel, P., H.Y. Shin, W.J. Emery and H. Grassl, 1987: Comparison of satellite-derived sea surface temperatures with in situ skin measurements, J. Geophys. Res., 92, 2859-2974.

Table 1.
Mooring Deployment, Recovery and Duration Times

Mooring ID	Deployment Time (UTC)	Recovery Time (UTC)	Duration (days)
F2	15 January '86 2020	14 June '86 0950	150
F4	16 January '86 1947	15 June '86 2133	150
F6	26 January '86 1715	14 June '86 2151	139
F8	27 January '86 1748	15 June '86 1333	139
F10	01 February '86 1801	10 June '86 0545	103 on station[1] 129 total[2]
F3	17 January '86 1811	16 June '86 1352	150
F5	18 January '86 1840	16 June '86 2011	149
F7	28 January '86 1852	17 June '86 1108	140
F9	29 January '86 1806	Lost	
F1	28 October '84 2238	18 June '86 1721	598
F12	29 October '84 1724	13 June '86 1957	592

[1] - Days on station before mooring line parted.
[2] - Days in operation; recovered 10 June 1986 off San Salvador Island in the Bahamas.

Table 2.
GPS/LORAN C Positions of Mooring Anchors

GPS Positions FASINEX Identifier	Visible Number	Latitude/Longitude	WHOI Mooring Designation
F2	A	27°18.95N 70°05.86W	845
F3		27°05.34N 69°42.75W	PCM-1
F4	C	27°05.35N 69°50.30W	846
F5		26°58.58N 69°50.40W	PCM-2
F6	B	27°12.59N 69°58.48W	847
F7		27°12.53N 69°51.03W	PCM-3
F8	E	26°58.66N 69°43.19W	848
F9		27°05.45N 69°58.33W	PCM-4
F10	D	27°19.63N 69°42.52W	849
LORAN C positions			
F[1]		27°58.90N 69°58.80W	829
F12		25°29.10N 70°00.70W	830

Table 3

Images used for calculation of motion and image pairs:

Image #	Date (1986)	Time (UVT)	Pair #
1.	January 29	19:00	1
2.	January 30	18:00	1
3.	February 6	07:00	2
4.	February 6	19:00	2,3
5.	February 7	19:00	3,4
6.	February 8	07:00	4
7.	February 22	09:00	14
8.	February 22	21:00	14
9.	March 7	19:00	5
10.	March 8	19:00	5
11.	March 20	18:00	6
12.	March 21	18:00	6
13.	April 15	18:00	7
14.	April 16	07:00	7
15.	April 25	18:00	8
16.	April 26	07:00	8,9
17.	April 26	18:00	9
18.	May 2	07:00	10
19.	May 2	19:00	10
20.	May 13	19:00	11
21.	May 14	07:00	11
22.	May 20	08:00	12
23.	May 20	19:00	12
24.	May 29	08:00	13
25.	May 29	19:00	13

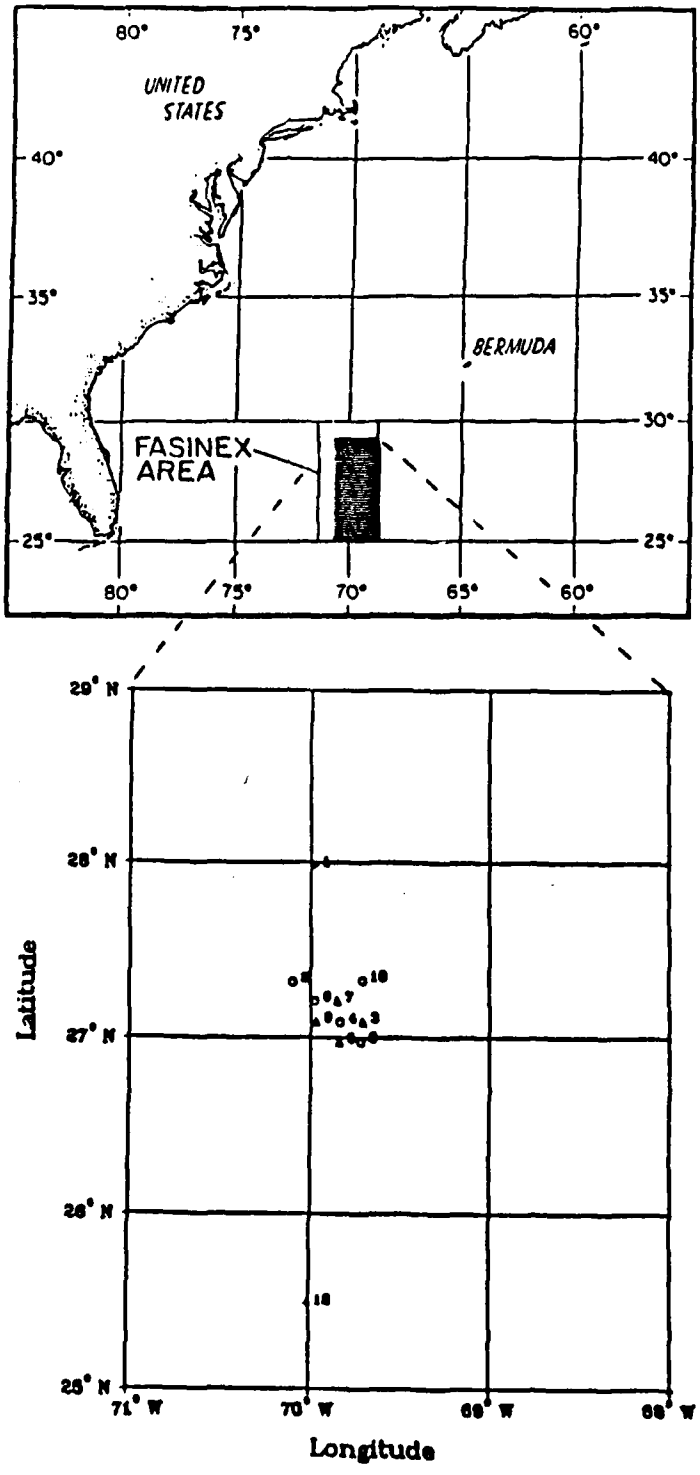

Figure 1 Geographic positioning of FASINEX moorings.

IMAGE #1

May 13, 1986 19:00 GMT (14:00 Local)

(2827 hours from January 15, 1986 00:00 GMT)

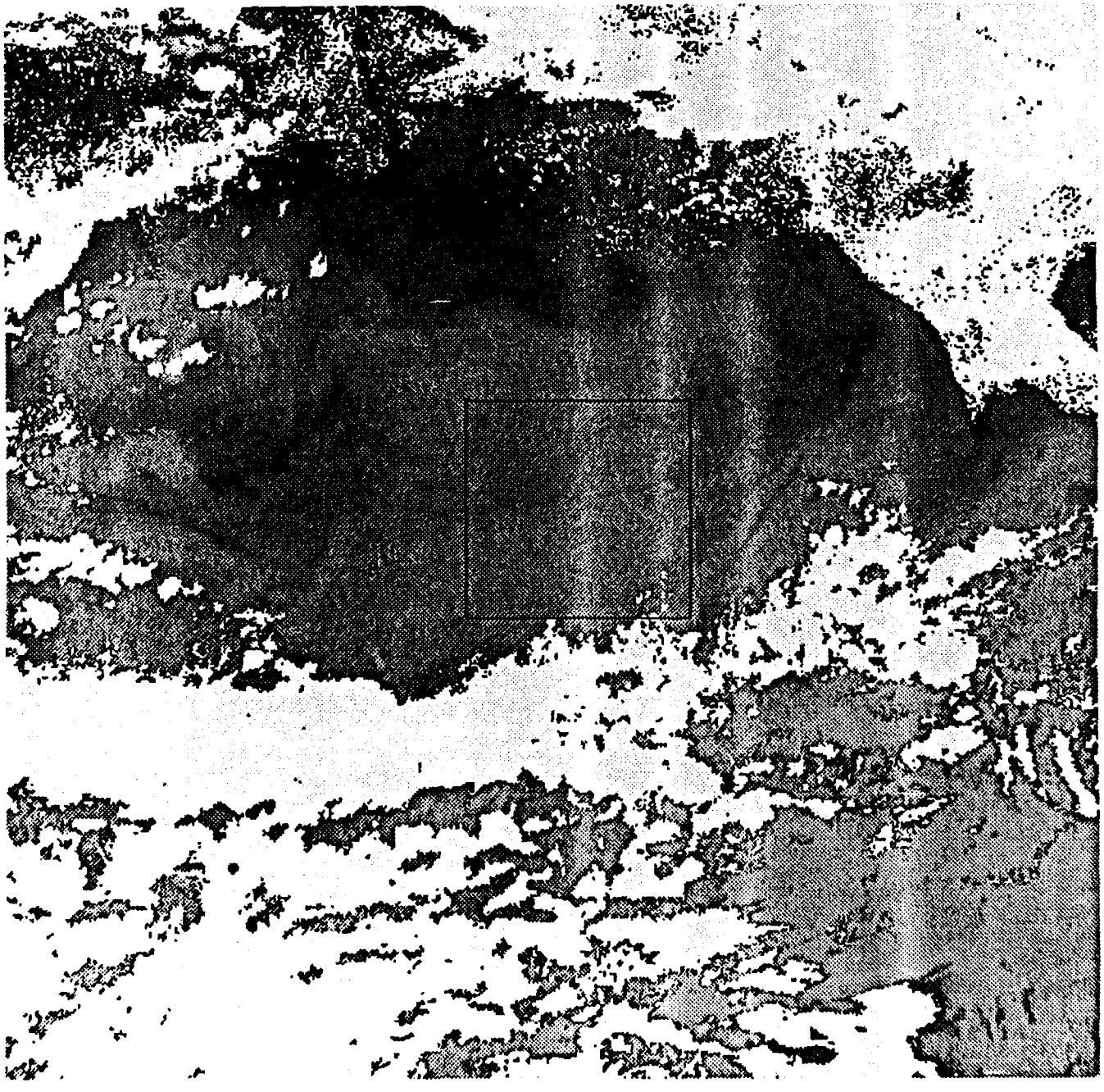

Fig. 2

IMAGE #2

May 14, 1986 07:00 GMT (02:00 Local)

(2839 hours from January 15, 1986 00:00 GMT)

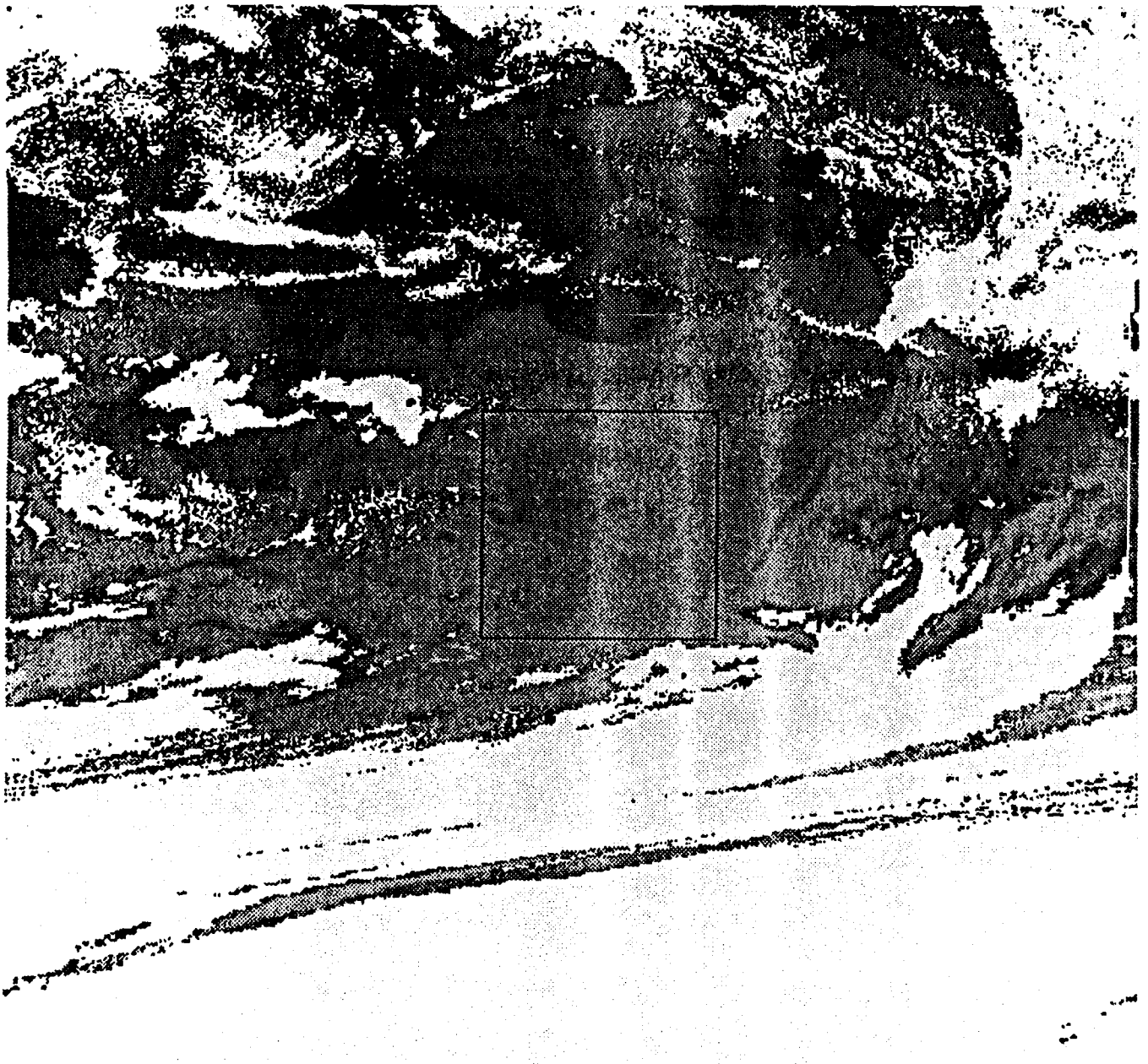

Fig. 3

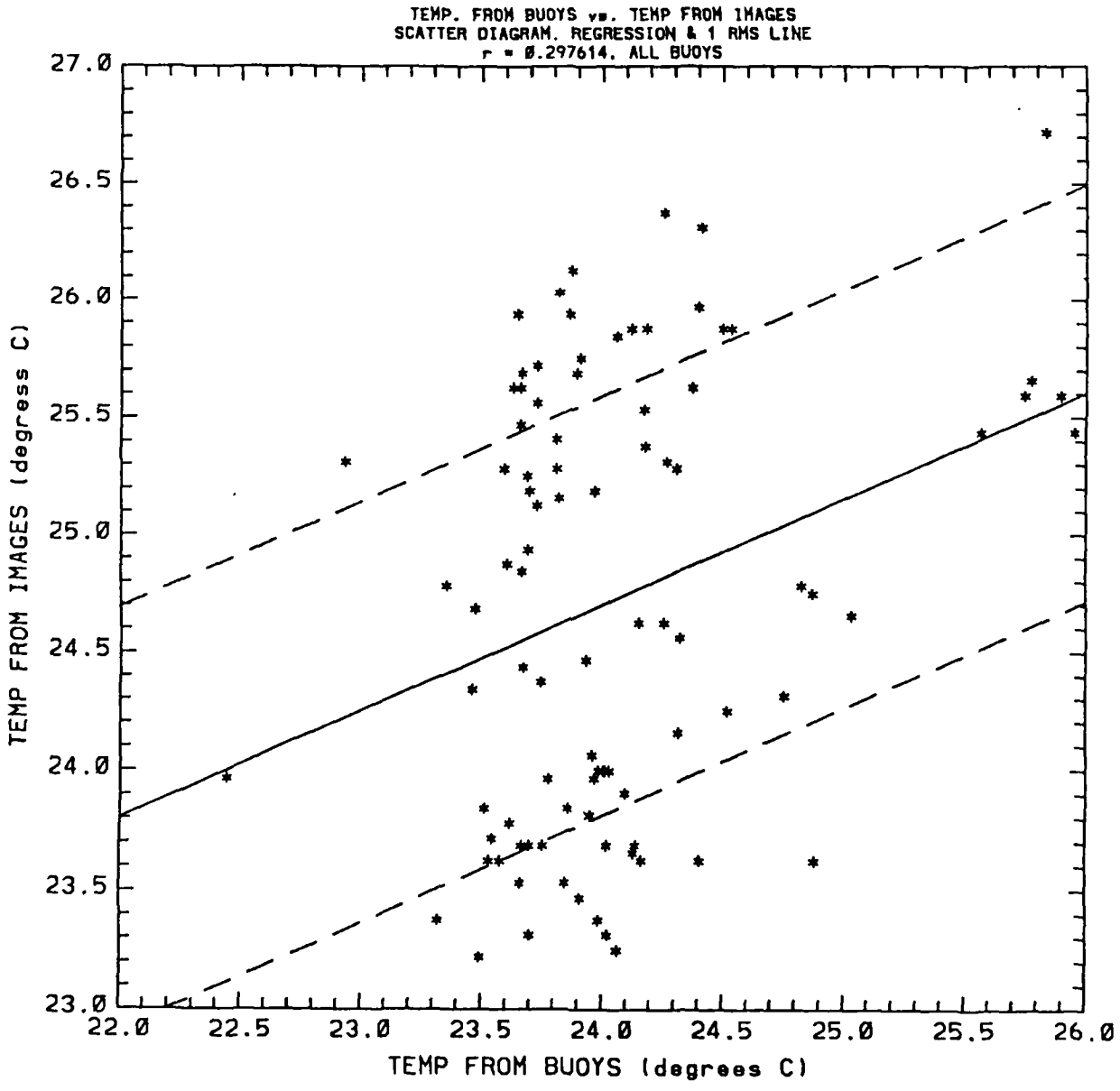
TEMP. FROM BUOYS vs. TEMP FROM IMAGES
SCATTER DIAGRAM. REGRESSION & 1 RMS LINE
r = 0.297614. ALL BUOYS
TEMP FROM IMAGES (degrees C)
TEMP FROM BUOYS (degrees C)
27.0
26.5
26.0
25.5
25.0
24.5
24.0
23.5
23.0
22.0
22.5
23.0
23.5
24.0
24.5
25.0
25.5
26.0

Fig. 4

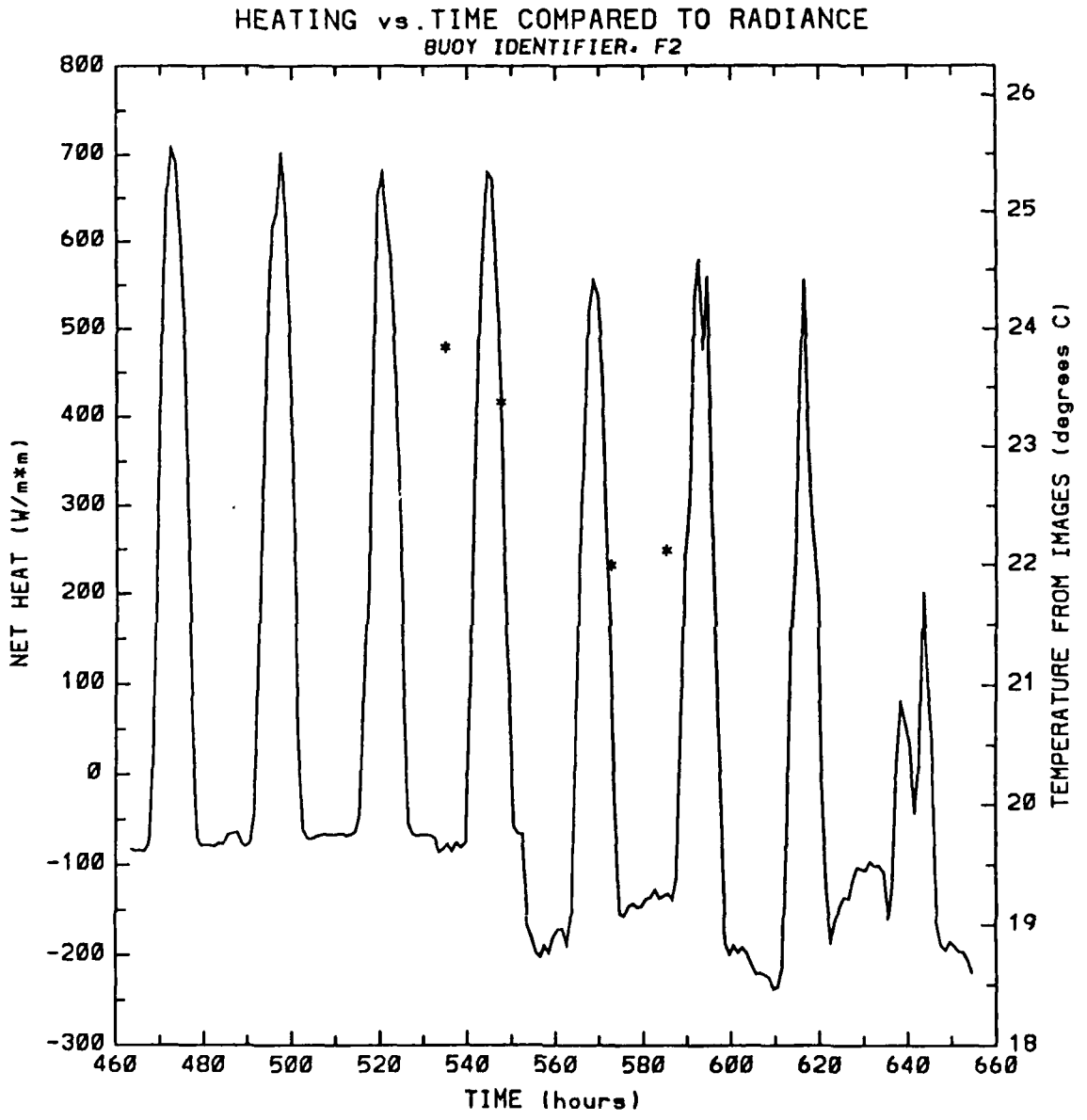
HEATING vs.TIME COMPARED TO RADIANCE
BUOY IDENTIFIER. F2
NET HEAT (W/m*m)
TEMPERATURE FROM IMAGES (degrees C)
TIME (hours)
800
700
600
500
400
300
200
100
0
-100
-200
-300
26
25
24
23
22
21
20
19
18
460
480
500
520
540
560
580
600
620
640
660

Fig. 5

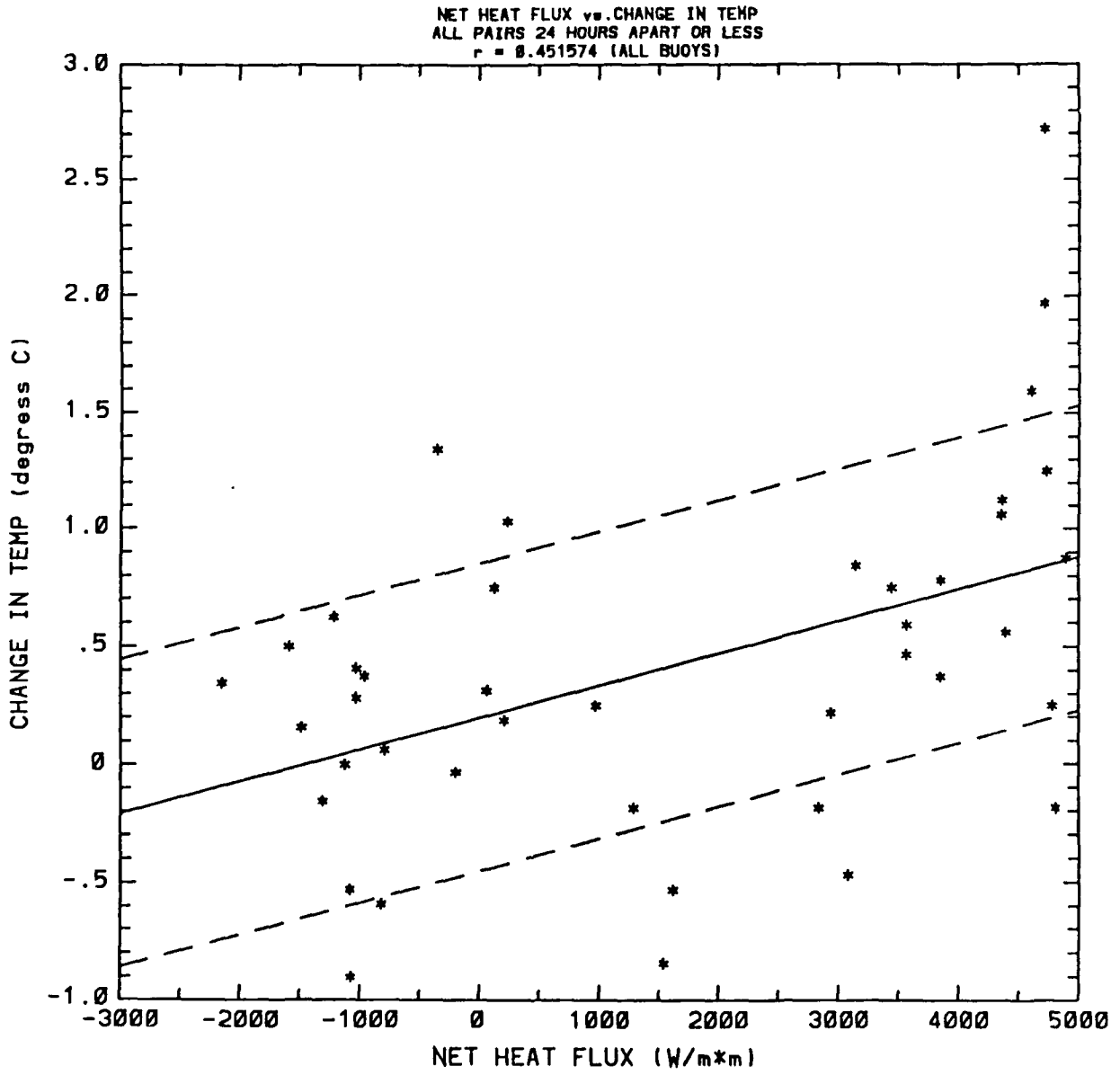
NET HEAT FLUX vs.CHANGE IN TEMP
ALL PAIRS 24 HOURS APART OR LESS
r = 0.451574 (ALL BUOYS)
CHANGE IN TEMP (degress C)
3.0
2.5
2.0
1.5
1.0
.5
0
-.5
-1.0
-3000
-2000
-1000
0
1000
2000
3000
4000
5000
NET HEAT FLUX (W/m*m)

Fig. 6

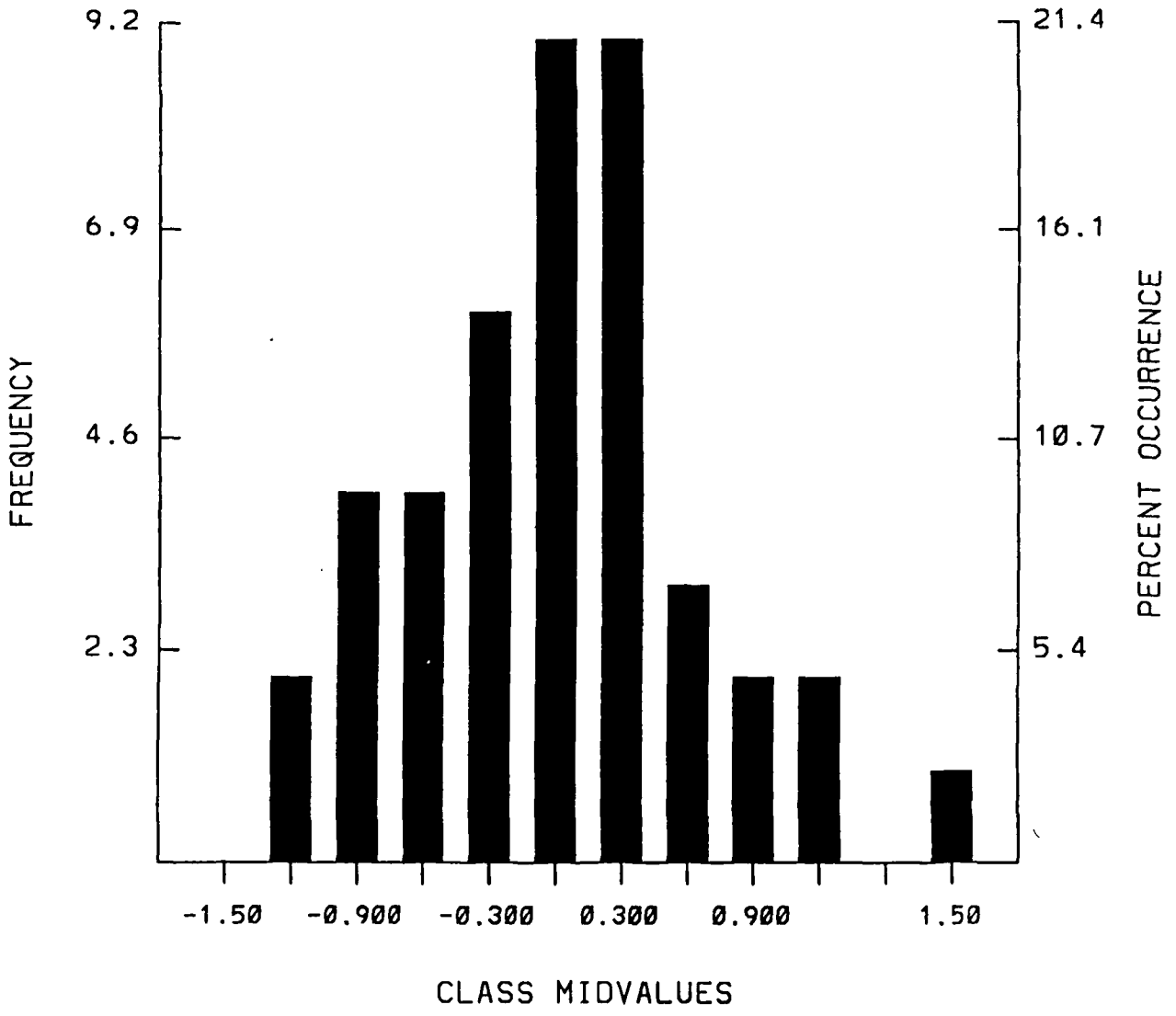
TEMPERATURE DISTANCE FROM REGRESSION LINE (Vertical)
9.2
6.9
4.6
2.3
FREQUENCY
21.4
16.1
10.7
5.4
PERCENT OCCURRENCE
-1.50
-0.900
-0.300
0.300
0.900
1.50
CLASS MIDVALUES

Fig. 7

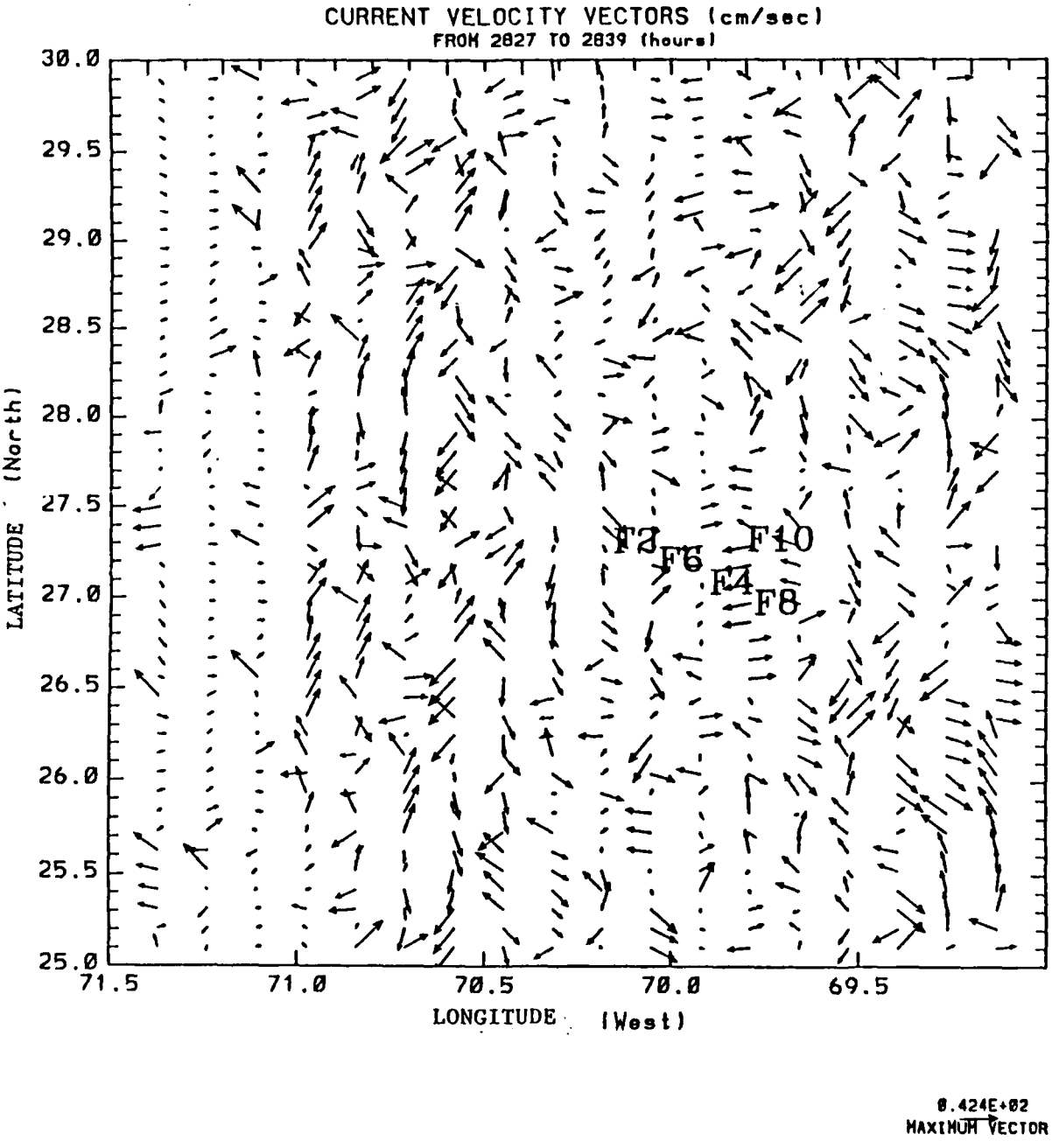
CURRENT VELOCITY VECTORS (cm/sec)
FROM 2827 TO 2839 (hours)
30.0
29.5
29.0
28.5
28.0
27.5
27.0
26.5
26.0
25.5
25.0
LATITUDE (North)
71.5
71.0
70.5
70.0
69.5
LONGITUDE (West)
F3
F6
F10
F4
F8
0.424E+02
MAXIMUM VECTOR

Fig 8